(12) INTERNATIONAL APPLICATION PUBLISHED UNDER THE PATENT COOPERATION TREATY (PCT)

(19) World Intellectual Property Organization
International Bureau

(43) International Publication Date
15 March 2012 (15.03.2012)

PCT

(10) International Publication Number
WO 2012/032117 A1

(51) International Patent Classification:
H01Q 15/00 (2006.01) *H01Q 17/00* (2006.01)

(21) International Application Number:
PCT/EP2011/065554

(22) International Filing Date:
8 September 2011 (08.09.2011)

(25) Filing Language: English

(26) Publication Language: English

(30) Priority Data:
10175887.8 9 September 2010 (09.09.2010) EP

(71) Applicants *(for all designated States except US)*: **UNIVERSITE CATHOLIQUE DE LOUVAIN** [BE/BE]; Place de l'Université 1, B-1348 Louvain-La-Neuve (BE). **UNIVERSITE DE LIEGE** [BE/BE]; Interface Entreprises-Université, Avenue Pré-Aily 4, B-4031 Angleur (BE).

(72) Inventors; and

(75) Inventors/Applicants *(for US only)*: **DETREMBLEUR, Christophe** [BE/BE]; rue d'Avister 6, B-4130 Esneux (BE). **MOLENBERG, Isabel** [BE/BE]; Avenue Paul Delvaux 8/311, B-1340 Ottignies (BE). **HUYNEN, Isabelle** [BE/BE]; Place des Peintres 9/102, B-1348 Louvain-La-Neuve (BE). **THOMASSIN, Jean-Michel** [BE/BE]; rue de la Waide 11, B-4670 Blegny (BE). **FURNEMONT, Quentin** [BE/BE]; avenue du Marouset 145, B-7090 Braine-Le-Comte (BE). **PARDOEN, Thomas** [BE/BE]; Clos de la Noire Epine 2, B-1435 Mont-Saint-Guibert (BE). **BAILLY, Christian** [BE/BE]; Koolkaai 1 bus 5, B-2000 Antwerpen (BE). **EGGERMONT, Stéphanie** [BE/BE]; avenue de Jemappes 86, B-7000 Mons (BE). **QUIEVY, Nicoals** [BE/BE]; avenue Charles Brassine 60/20, B-1160 Auderghem (BE). **URBANCZYK, Laetitia** [BE/BE]; rue Molinvaux 19, B-4000 Liege (BE).

(74) Agents: **PECHER, Nicolas** et al.; Centre Monnet, avenue Jean Monnet 1, B-1348 Louvain-La-Neuve (BE).

(81) Designated States *(unless otherwise indicated, for every kind of national protection available)*: AE, AG, AL, AM, AO, AT, AU, AZ, BA, BB, BG, BH, BR, BW, BY, BZ, CA, CH, CL, CN, CO, CR, CU, CZ, DE, DK, DM, DO, DZ, EC, EE, EG, ES, FI, GB, GD, GE, GH, GM, GT, HN, HR, HU, ID, IL, IN, IS, JP, KE, KG, KM, KN, KP, KR, KZ, LA, LC, LK, LR, LS, LT, LU, LY, MA, MD, ME, MG, MK, MN, MW, MX, MY, MZ, NA, NG, NI, NO, NZ, OM, PE, PG, PH, PL, PT, QA, RO, RS, RU, RW, SC, SD, SE, SG, SK, SL, SM, ST, SV, SY, TH, TJ, TM, TN, TR, TT, TZ, UA, UG, US, UZ, VC, VN, ZA, ZM, ZW.

[Continued on next page]

(54) Title: HYBRID MATERIAL FOR ELECTROMAGNETIC ABSORPTION

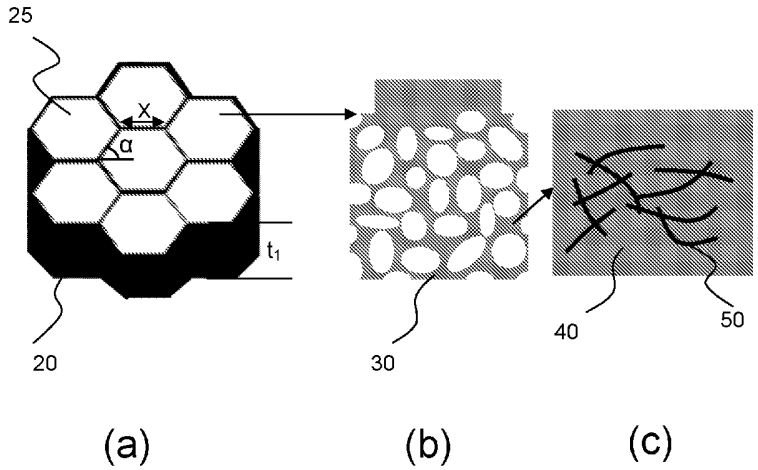

Fig. 2

(57) Abstract: The present invention relates to a hybrid material (10) for absorbing electromagnetic radiation (60) and a method for making such a material. The hybrid material (10) comprises at least one grid panel (20) of thickness t_1 having holes (25) traversing said thickness t_1, at least one polymer composite material (30) of thickness t_2 filling at least partially the holes (25) of the at least one grid panel (20), said at least one polymer composite material (30) including a polymer matrix (40) and conductive particles (50) dispersed into said polymer matrix (40), characterized in that the internal surface of the holes (25) of the at least one grid panel (20) is metallic.

WO 2012/032117 A1

(84) **Designated States** *(unless otherwise indicated, for every kind of regional protection available)*: ARIPO (BW, GH, GM, KE, LR, LS, MW, MZ, NA, SD, SL, SZ, TZ, UG, ZM, ZW), Eurasian (AM, AZ, BY, KG, KZ, MD, RU, TJ, TM), European (AL, AT, BE, BG, CH, CY, CZ, DE, DK, EE, ES, FI, FR, GB, GR, HR, HU, IE, IS, IT, LT, LU, LV, MC, MK, MT, NL, NO, PL, PT, RO, RS, SE, SI, SK, SM, TR), OAPI (BF, BJ, CF, CG, CI, CM, GA, GN, GQ, GW, ML, MR, NE, SN, TD, TG).

Published:

— *with international search report (Art. 21(3))*

HYBRID MATERIAL FOR ELECTROMAGNETIC ABSORPTION

TECHNICAL FIELD

[0001] The present invention relates generally to the field of electromagnetic absorption. In particular, the invention relates to a hybrid material for absorbing electromagnetic radiation and a method for making such a material.

DESCRIPTION OF RELATED ART

[0002] Electromagnetic pollution is a subject of worldwide preoccupation regarding potentially harmful health issues and proper operation of a wide range of electrical devices. Indications of potential health problems due to electromagnetic pollution are indeed sometimes related (see for instance the article by Adang D. et al., entitled “Results of a long-term low-level microwave exposure of rats” in IEEE Transactions on Microwave Theory and Techniques, 57, 2488-2497 (2009)). Electromagnetic interferences (EMI) can also have dramatic consequences on the functioning of electrical devices such as in medical or airspace applications.

[0003] In some situations, a simple metallic foil is sufficient to reflect an incident electromagnetic wave and to preserve the electrical integrity of a system, or to avoid the electromagnetic radiations to escape the system.

[0004] In a series of applications, true absorption of the electromagnetic radiation, at least from one side of an interface, is recommended and sometimes mandatory. For some electronic circuits, the self reflection of the waves can be detrimental on proper operation. True electromagnetic absorption is also required in anechoic chambers for testing electronic devices, antennas and the like and in stealth military applications (naval or air crafts than cannot be detected).

[0005] Absorption of electromagnetic waves requires preventing both reflection of the incident wave and transmission of the wave through the medium. The absorbed power P_a is given by equation (Eq. 1):

$$P_a = P_i - P_r - P_{out} \quad \text{(Eq. 1)},$$

where P_i is the incident power, P_r is the reflected power, and P_{out} is the transmitted power. The absorption is quantified by the absorption index

$$A = P_a/P_i \quad \text{(Eq. 2)}.$$

[0006] Figure 1 shows a semi-infinite slab 70 of thickness t that is subjected to a normally incident electromagnetic radiation 60 of frequency *f*. At each side of the slab (z < 0, z > t), the medium is air. In such a case, one can calculate the absorption index A of equation (Eq. 2) carried out by the slab by using transmission line formalism and by imposing the required conditions of continuity of the electric and magnetic field at the interfaces of the slab. The result of such a calculation is given in equation (Eq. 3):

$$A = 1 - \left|\frac{\Gamma\left(T^2-1\right)}{1-\Gamma^2T^2}\right|^2 - \left|\frac{T\left(1-\Gamma^2\right)}{1-\Gamma^2T^2}\right|^2 \quad \text{(Eq. 3)}$$

where the reflection coefficient

$$\Gamma = \left(\sqrt{\varepsilon_{eff}} - 1\right)/\left(\sqrt{\varepsilon_{eff}} + 1\right) \quad \text{(Eq. 4)}$$

and the transmission coefficient

$$T = \exp\left(-j\omega t\sqrt{\varepsilon_{eff}}/c_0\right) = \exp(-\gamma_c t) \quad \text{(Eq. 5)}$$

are function of the dielectric constant ε_r and electrical conductivity σ of the slab entering in the definition of the complex effective dielectric constant of the slab : $\varepsilon_{eff} = \varepsilon_r - j\sigma/\omega\varepsilon_0$. The pulsation ω is given by the equation $\omega = 2\pi f$, c_0 is the speed of light in air, *j* is the imaginary number, and

$$\gamma_c = j\sqrt{\varepsilon_{eff}}\,\omega/c_0 \quad \text{(Eq. 6)}$$

is the complex propagation constant in the slab.

[0007] For a given thickness and frequency, the absorption index *A* of equation (Eq. 2) can be calculated for all existing materials based on known material properties data by using equation (Eq. 3). From such calculations, one can deduce that the best absorbing materials combine a dielectric constant ε_r as close as possible to 1 and a moderately high electrical conductivity σ around 1 S/m. No existing simple material is found in this optimum area. Metals present a large conductivity such that the norm of the reflection coefficient $|\Gamma|$ is almost equal to 1 and the electromagnetic wave is entirely reflected. The best possibilities of single materials are, in principle, leather and plaster of Paris but these two materials do not present sufficiently high absorption indices for moderate thickness.

[0008] Composite materials emerge naturally as the solution when seemingly antagonist properties are required as in the present case involving a low dielectric constant (around 1) and moderately high conductivity (around 1 S/m). Most polymers are electrical insulators such that they are transparent to electromagnetic radiations. Reinforcing polymers with carbon based conductive loads such as carbon fillers, carbon nanotubes (CNT), carbon black or a mixture thereof constitutes an attractive option to reach the expected level of conductivity, around 1 S/m, at high frequency (see for instance the article by A. Saib et al. Entitled "Carbon nanotube composites for broadband microwave absorbing materials", in IEEE Transactions on Microwave Theory and Techniques, 54, 2745-2754 (2006) or EP 1 947 923 that discloses an electromagnetic wave absorber where carbon fibrous structures are contained in a matrix). However, the dielectric constant is also increased by the incorporation of carbon based particles, which has a detrimental impact on the reflectivity of the materials. In order to benefit from the conductivity of the carbon based conductive loads while not increasing too much the dielectric constant, one can introduce open space to the material. Foaming is thus very effective to limit the detrimental impact of carbon loads on the dielectric. The strategy of combining a foam polymer with CNT is notably illustrated in the article by J.-M. Thomassin et al. entitled "Foams of polycaprolactone / MWNT nanocomposites for efficient EMI reduction", in Journal of Materials Chemistry, 18, 792-796. However, the dielectric constant of such materials is still too large

to obtain high absorption.

[0009] Salisbury screens are well-known by the persons skilled in the art as panels for strongly decreasing the reflection of an incident electromagnetic wave. When such a radiation strikes the surface of the panel, it is split into two waves of equal intensity thanks to the use of a specific layer. The first wave is reflected on the external surface of the panel whereas the second wave passes through a dielectric layer before being reflected by a second surface. The thickness of the dielectric layer is chosen to be equal to a quarter of the wavelength of the frequency of the electromagnetic radiation. The extra distance the second wave travels causes it to be 180° out of phase with the first wave. When the second wave reaches the external surface of the panel, the two waves combine and cancel each other. Therefore, there is no electromagnetic energy that is reflected by the panel. The first disadvantage of Salisbury screens is that they work well only at a single frequency. Multilayer Salisbury designs can cover a band of frequencies, but only by increasing the thickness, and the best cover only a fraction of the frequency spectrum. Another problem is the thickness of the screen itself. If one wants to have a screen that strongly decreases the reflection of an electromagnetic radiation of frequency f=1 GHz as an example, one has to use a dielectric layer having a thickness equal to 7.5 cm.

[0010] Therefore, there is a need for a material (and a method for making it) that presents a dielectric constant ε_r around 1 and a moderately high conductivity σ around 1 S/m resulting in high power of absorption and low power of reflection of an incident electromagnetic radiation. Preferentially, this material should also have a tunable thermal conductivity, high or low depending on the need, such a property being critical for electronic or housing applications, should be light and able to withstand mechanical deformations.

SUMMARY OF THE INVENTION

[0011] The present invention relates to a hybrid material that efficiently absorbs electromagnetic radiation and to a method for making such a material.

[0012] According to a first aspect of the invention, a hybrid material is provided that comprises at least one grid panel of thickness t_1 having holes

traversing said thickness t_1, at least one polymer composite material of thickness t_2 filling at least partially the holes of the at least one grid panel, said at least one polymer composite material including a polymer matrix and conductive particles dispersed into said polymer matrix, characterized in that the internal surface of the holes of the at least one grid panel is metallic.

[0013] In a first embodiment, the thickness t_2 of the at least one polymer composite material filling at least partially the holes of the at least one grid panel is smaller than the thickness t_1 of the at least one grid panel.

[0014] Preferably, the shape of the holes traversing the thickness t_1 of the grid panel is a prism with a hexagonal base.

[0015] In another embodiment, the conductive particles dispersed into the polymer matrix of the at least one polymer composite material are carbon based conductive loads.

[0016] A further development of the hybrid material is characterized in that the carbon based conductive loads comprise carbon based fillers, carbon nanotubes, carbon black or a mixture thereof.

[0017] When carbon nanotubes are chosen as carbon based conductive loads, one could preferably choose to position them in such a manner that their axes are perpendicular to the thickness t_1 of the at least one grid panel.

[0018] In another embodiment, the at least one grid panel is metallic.

[0019] In still another embodiment, the at least one grid panel (20) is not metallic and the internal surface of the holes of the grid panel is metalized.

[0020] A still further development of the hybrid material is characterized in that the lateral surfaces of said hybrid material are covered by additional sheets of materials whereby the bending stiffness and / or the mechanical strength of the resultant panel are increased.

[0021] One can advantageously tailor the size of the holes of the grid panel in order to improve the absorption of an incident electromagnetic radiation in a range of frequency

[0022] Another possibility to improve the absorption of an incident electromagnetic radiation in a range of frequency is to deform the hybrid material.

[0023] In still another embodiment, the at least one polymer composite material is a foam.

[0024] When the at least one polymer composite material is a foam, one could prefer to use a foam that presents a gradient of foam density.

[0025] A still further development is characterized in that the hybrid material further comprises at least one dielectric layer between said hybrid material and at least one additional hybrid material.

[0026] When the hybrid material further comprises at least one dielectric layer between said hybrid material and at least one additional hybrid material, one could preferably choose a dielectric layer that comprises a polymer matrix.

[0027] According to a second aspect of the invention, a process for making a hybrid material that absorbs an electromagnetic radiation is provided. In a first embodiment the method includes the steps of: forming a polymer composite material by dispersion of particles in a melt polymer matrix or by a co precipitation process, inserting a grid panel of thickness t_1 having holes traversing said thickness t_1 in the polymer composite material, optionally foaming the composite material before or after the step of insertion of the grid panel.

[0028] In a second embodiment the method includes the steps of: casting in a grid panel of thickness t_1 having holes traversing said thickness t_1 reactants that are monomers, solvent, particles, catalyst or polymerization initiator, exposing the set obtained in the first step to polymerization conditions, optionally foaming the resultant material.

BRIEF DESCRIPTION OF THE DRAWINGS

[0029] Fig.1 shows an electromagnetic radiation that is normally incident to a semi-infinite slab of thickness t.

[0030] Fig.2 shows a preferred embodiment of the hybrid material of the invention. Fig. 2(a) represents a grid panel when the holes have the shape of a prism with a regular hexagonal base. Fig. 2(b) relates to the polymer composite material filling the holes of the grid panel when said polymer composite material has a foam structure. Fig. 2(c) is a zoom inside the polymer composite material comprising a polymer matrix and conductive particles when said conductive particles are carbon nanotubes (CNT).

[0031] Fig.3 shows the frequency variation of the measured absorption

index *A* per unit thickness of a hybrid material of the invention and of a polymer composite material alone.

[0032] Fig.4 shows the frequency variation of the calculated absorption index *A* per unit thickness of a hybrid material of the invention and of a polymer composite material alone.

[0033] Fig.5 shows the frequency variation of the calculated dielectric constant of a hybrid material of the invention and of a polymer composite material alone.

[0034] Fig.6 shows the frequency variation of the measured reflection index *R* of a hybrid material of the invention and of a polymer composite material alone.

[0035] Fig.7 shows the frequency evolution around 30 GHz of the calculated absorption index *A* of a hybrid material and of a polymer composite material alone when the thickness of the corresponding slabs is equal to 3 cm.

[0036] Fig.8 shows the measured evolution of the absorption index *A* in percent with frequency of a hybrid material of the invention and of a polymer composite material alone when said polymer composite material has a thickness t_2 that is smaller than the thickness t_1 of the grid panel.

[0037] Fig.9 shows the geometries used with the Finite-Element simulations. Fig.9(a) represents the used geometry when the simulations consider that the absorbing slab only comprises a polymer composite material. Fig.9(b) shows the used geometry when the absorbing slab is made of a hybrid material according to the invention.

[0038] Fig.10 shows the results of the analytical calculations and of the Finite-Element simulations for the variation of the absorption index *A* (in percent) with respect to frequency when the electrical conductivity of the polymer composite material is equal to 0.5 S/m. The thickness of the slab is equal to 5 mm and both calculations are carried out for a hybrid material according to the invention and for a polymer composite material alone.

[0039] Fig.11 shows the results of the analytical calculations and of the Finite-Element simulations for the variation of the absorption index *A* (in percent) with respect to frequency when the electrical conductivity of the polymer composite material is equal to 1 S/m. The thickness of the slab is equal to 5 mm and both calculations are carried out for a hybrid material

according to the invention and for a polymer composite material alone.

[0040] Fig.12 shows the calculated reflection index *R* (in decibels) versus frequency of a hybrid material according to the invention and of a polymer composite material alone.

[0041] Fig.13 shows the results of the analytical calculations and of the Finite-Element simulations for the variation of the absorption index *A* (in percent) with respect to frequency when the electrical conductivity of the polymer composite material is equal to 0.5 S/m. The thickness of the slab is equal to 10 mm and both calculations are carried out for a hybrid material according to the invention and for a polymer composite material alone.

[0042] Fig.14 shows the frequency evolution of the absorption capabilities of a hybrid material according to the invention when said hybrid material is deformed.

[0043] Fig.15 shows at several frequencies the value of the performance index M_1 for different materials for which the absorption index *A* has been fixed to 90 %.

[0044] Fig.16 presents the frequency evolution of the performance index M_2 versus frequency for different materials for which the absorption index *A* has been fixed to 90 %.

[0045] Fig.17 represents the equivalent circuit of the hybrid material.

[0046] Fig.18 represents the equivalent circuit of a material comprising at least two hybrid materials separated by a dielectric layer.

[0047] Fig.19 shows the calculated absorption index *A* versus frequency carried out by a hybrid material of the invention and by a material composed of fifteen hybrid materials, each separated by a dielectric layer.

DETAILED DESCRIPTION OF THE INVENTION

[0048] Explanation will be given in detail with reference to the drawings. To obtain efficient absorbing materials, one could think of a polymer material including conductive particles such as carbon fillers, carbon nanotubes (CNT), carbon black or a mixture thereof. The problem would then to decrease the dielectric constant ε_r of the resulting polymer composite material 30 in order to decrease its reflection power.

[0049] Referring to figure 2, the inventors have found that inserting a specific grid panel 20 into such a polymer composite material 30 reduces the dielectric constant ε_r of the resulting material over the whole electromagnetic spectrum, ε_r being even equal to 1 in a specific frequency range which leads to an efficient absorbing material. To obtain such an absorbing material, the inventors propose to combine the wave guide properties of the grid panel 20 and the dissipative properties of the polymer composite material 30. The grid panel 20 has a thickness t_1 and holes 25 traversing said thickness t_1. The grid panel 20 presents good wave guide properties if the internal surface of the holes 25 is composed of a material presenting a very high electrical conductivity, which means an electrical conductivity σ that is equal or higher than 10^6 S/m at 20 °C (293.15 K). So, to obtain the material of the invention, that we name hybrid material 10, one needs to use a grid panel 20 such that the internal surface of the holes 25 of said grid panel 20 is metallic. Examples of metals that can be used for the internal surface of the holes 25 of the grid panel 20 are silver, aluminium, gold, copper or other metals having a high electrical conductivity. Inserting a grid panel in a polymer charged with conductive particles has been notably proposed in the article by H Yanfei et al. entitled “Preparation and microwave absorption properties of foam-based honeycomb sandwich structures” in Europhysics Letters 85 (2009), 58003. In this case, the internal surface of the holes of the grid panel is not metallic as it is suggested in the end of the first paragraph of page 4 of this article. The article published in Composites Science and Technology 67 (2007), 3472, by H.L. Fan and entitled “Microwave absorbing composite lattice grids” also proposes a material comprising a lattice grid and spongy foam materials including carbon particles. In this last article, the lattice grid can be reinforced by carbon fibers. Such a grid is then conductive but the maximum electrical conductivity that can be expected for such a grid at 20 °C is 10^4 S/m. Such a value is not enough to obtain a grid presenting efficient wave guide properties. In these two examples, the grid panel is only used to enhance the mechanical properties of the resulting material. The grid panel 20 of the hybrid material 10 of the invention is used for its waveguide properties. By combining these wave guide properties with the dissipative properties of the polymer composite

material 30, the inventors have obtained a material that efficiently absorbs an electromagnetic radiation, with advantageously combining other mechanical and thermal properties.

[0050] Figure 2 shows a preferred embodiment of the hybrid material 10 of the invention. Such a hybrid material 10 comprises a grid panel 20 having a thickness t_1 and holes 25 traversing said thickness t_1 (see figure 2(a)) and a polymer composite material 30 having a thickness t_2. A cross-section of the polymer composite material 30 that fills the holes 25 of the grid panel 20 is shown in figure 2(b). One can choose to have $t_2 = t_1$, $t_2 < t_1$ or $t_2 > t_1$. So, the holes 25 of the grid panel 20 can be only partially filled by the polymer composite material 30. The embodiment corresponding to $t_2 < t_1$ allows one to use the unfilled portion of the grid panel 20 as a reflective protection when such an unfilled portion is placed at the exit of the hybrid material 10. Then, the part of the electromagnetic radiation 60 that is not be absorbed by the polymer composite material 30 during its first crossing of the hybrid material 10 is reflected by the unfilled part of the grid panel 20 and undergoes a second absorption during its backward crossing into the polymer composite material 30. In figure 2(a), the grid panel 20 has the form of a honeycomb lattice, which means that the holes 25 have the form of a prism with a regular hexagonal base, but other shapes could be used (square holes, circular holes, irregular polygons). In the case of a honeycomb lattice, the angle α depicted in figure 2(a) is equal to 60 °. The parameter X in figure 2(a) represents the size of a side of a hexagonal hole of the honeycomb lattice. Only the internal surface of the holes 25 of the grid panel 20 needs to be metallic. So, one can use for instance a non-metallic grid panel 20 if the internal surface of the holes 25 of the grid panel 20 is covered by a metallic layer. Such a metallic layer can be deposited by any suitable chemical or physical deposition method (sputtering, electrochemical deposition methods are two possible examples). In applications requiring a good thermal dissipation, one would rather choose a metallic grid panel 20. The inventors have notably used an aluminium grid panel 20 because of its combined properties of lightness and stiffness. Such grid panels 20 can be purchased or made by conventional techniques used for producing honeycomb lattices (extrusion as an example).

[0051] The holes 25 of the honeycomb lattice of figure 2(a) are filled at

least partially along the thickness t_1 with a polymer composite material 30 that is shown in figure 2(b). The composite polymer material 30 comprises a polymer matrix 40 and conductive particles 50 that are dispersed into said polymer matrix 40 (see figure 2(c)). All known polymer material can be used for the polymer matrix 40. As an example, the polymer matrix 40 can be selected from the group consisting of polylactic acid, polyglycolic acid, poly(ε-caprolactone), polyhydroxyalkanoate, polyacrylates, polymethacrylates, polyurethanes, polycarbonates, polyamides, polyetheretherketones, polyvinylalcohols, polyesteramines, polyesteramides, polysulfones, polyimides, polyethyleneglycol, fluronated polymers, polystyrene and derivatives, or mixtures thereof.

[0052] As polymer materials are electrical insulators and then transparent to electromagnetic radiations, conductive particles 50 are dispersed into the polymer matrix 40. Different types of conductive particles 50 can be used and mixed. The only requirement is that such particles have a much higher electrical conductivity than the polymer matrix 40. As an example, one can use: copper, silver, aluminium, carbon based particles or a mixture thereof. Carbon based particles can have the form of carbon based fillers, carbon nanotubes (CNT), carbon black. A few percent of CNT has indeed shown to raise electrical conductivity of the resulting charged polymer at high frequency owing to virtual connections created by electrical capacitances existing between closely spaced nanotubes. When CNT are used as conductive particles 50, one could preferably choose to align them in such a way that their axes are perpendicular to the thickness t_1 of the grid panel 20. Indeed, the predominant propagation mode does not have typically any component of the electric field along the thickness t_1 of the grid panel 20.

[0053] In figure 2(b), the composite polymer material 30 has a foam structure. Such a structure allows one to limit the increase of the dielectric constant ε_r of the polymer composite material 30 after the incorporation of the conductive particles 50 such as CNT and to decrease the weight of the hybrid material 10. Although a foam structure for the polymer composite material 30 is preferred to induce a decrease of reflection of an incident electromagnetic radiation 60, such a structure is not necessary in the present invention. In order to further decrease the power of reflection of the hybrid material 10, one can

impose a gradient of the foam density along the thickness t_2 of the polymer composite material 30. Such a gradient would indeed induce a more progressive variation of the dielectric constant of the material traversed by an electromagnetic radiation 60 which results in lower reflections.

[0054] There are two main different processes to make the hybrid material 10 of the invention. First, the grid panel 20 can be inserted in the polymer composite material 30 that is already formed, for example by heating the grid panel 20 and/or the polymer composite material 30 and by pressing to the grid panel 20 for its insertion in the polymer composite material 30. If a foamed polymer composite material 30 is wanted, the foaming process can be applied after or before the insertion of the grid panel 20. Foams can be obtained by using supercritical carbon dioxide or by using classical foaming agents. All known methods by persons skilled in the art can be used for the preparation of the polymer composite material 30. In particular, the conductive particles 50 can be dispersed in the melt polymer matrix 40 or by a co precipitation process. Second, the preparation of the polymer composite material 30 can be carried out in the grid panel 20 itself. A liquid mixture including the required reactants is then casted in the grid panel 20 and exposed to polymerization conditions to obtain the polymer composite material 30. After, a foaming process can be applied if requested.

[0055] We now detail a process of fabrication of the hybrid material 10 when the grid panel 20 is inserted in the polymer composite material 30 that is already formed. More specifically, we focus on the case where the polymer composite material 30 is a foamed structure that comprises a polyurethane (TPU) or poly(ε-caprolactone) matrix and carbon nanotubes (CNT). Samples prepared by this technique were used for evaluating the absorbing capabilities of the hybrid material 10 of the invention. Polyurethane (PU, Desmopan® 2590A, Bayer) or poly(ε-caprolactone) (PCL, CAPA6500, Perstorp UK) is melt blended with 1 or 2 wt% of multiwalled carbon nanotubes (Nanocyl 7000, 90%) in a counter-rotating twin-screw static mixer (Brabender®) at 180°C (PU) or 100°C (PCL) for 5 min at 60 rpm. The polymer composite material 30 is then pressed for 5 min in a hot press at 180°C (PU) or 100°C (PCL) in order to obtain ready-to-foam 4 mm-thick sheets. The sheets are then placed in a high pressure vessel at 60°C (PU) or 50°C (PCL) and the vessel is then pressurized

with CO_2 (99.5%, Air Liquide, Belgium) at 250 bar (ISCO pump) for 24h in order to ensure equilibrium of saturation. The pressure is then released within 30 s. PCL composites foam under these conditions, while saturated PU-based sheets are quickly transferred between two hot plates at 120°C for two minutes to induce foaming. The foams are finally quenched in an ice/water bath. Finally, an aluminium honeycomb lattice (Liming HoneycombComposites Co., Ltd., China), forming 6 mm-sided hexagons, is incorporated in the composite foam mechanically after heating at 220°C (PU) or 120°C (PCL) in an oven. The heated honeycomb is slowly penetrated into the foam by manual pressing.

[0056] A sample that we name sample 1 and that has been prepared by the technique described in the previous paragraph was inserted in a measurement setup to evaluate its power of absorption. The honeycomb lattice that represents the grid panel 20 has a thickness t_1 equal to 5 mm and the polymer composite material 30 comprises a polyurethane foam matrix with a concentration of 2 wt% of CNT. For sample 1, the thickness t_2 of the polymer composite material 30 is equal to t_1 and said polymer composite material 30 fills the holes 25 of the grid panel 20 all along the thickness t_1. The reflection and absorption characteristics have been measured by using a Vector Network Analyser Model Wiltron 360. A set of calibration measurements has been primarily performed in order to remove the influence of connectors. Figure 3 shows the measured absorption index per unit thickness in percent *A/mm* versus frequency. The solid curve represents the absorption index of sample 1 (hybrid material 10 of the invention) whereas the dashed curve has been obtained with the same polymer composite material 30 as sample 1 but without the grid panel 20. The curve discontinuities are due to changes of the measurement probe in the different frequency intervals. We observe that the absorption carried out by sample 1 (hybrid material 10) is larger than the absorption carried out by the polymer composite material 30 alone in a range of frequency. More specifically, the absorption index of the hybrid material 10 presents a peak at 6.6 GHz.

[0057] By using equation (Eq. 3), one can calculate the absorption index *A* of the hybrid material 10. Then, one needs to know its complex effective dielectric constant $\varepsilon_{\mathrm{eff,h}}$. By using the equations of propagation of an electromagnetic wave in a waveguide filled with a material having a complex

effective dielectric constant $\varepsilon_{\text{eff,c}}$ (the polymer composite material 30 in our case), one can calculate the complex propagation constant of the hybrid material, γ_h.

[0058] For a metallic grid panel having rectangular holes with side lengths equal to *a* and *b*, one can use canonical expressions of waveguides to obtain the complex propagation constant of the hybrid material:

$$\gamma_h = j\sqrt{\varepsilon_{\text{eff,c}}\,\frac{\omega^2}{c_0^2} - \left(\frac{m\pi}{a}\right)^2 - \left(\frac{n\pi}{b}\right)^2} \quad \text{(Eq. 7)}$$

where *n* and *m* are integers representing different modes of propagation in the metallic grid. By identifying this expression with the expression of $\gamma_c = j\omega\sqrt{\varepsilon_{eff}}/c_0$, one can deduce the complex effective dielectric constant of the hybrid material, $\varepsilon_{\text{eff,h}}$. For a hybrid material including a metallic grid panel with rectangular holes, one then has

$$\varepsilon_{\text{eff,h}} = \varepsilon_{\text{eff,c}} - \left[\left(\frac{m\,\pi}{a}\right)^2 + \left(\frac{n\,\pi}{b}\right)^2\right]\left(\frac{c_0}{w}\right)^2 = \varepsilon_r\left(1 - \frac{\omega_0^2}{\omega}\right) - j\,\sigma/\omega\varepsilon_0 \quad \text{(Eq. 8)},$$

where $\omega_0 = 2\pi f_0$, f_0 being the cut-off frequency, and where ε_r entering equation (Eq. 8) is the dielectric constant of the polymer composite material 30. Equation (Eq. 8) reveals that the equivalent dielectric constant seen by the wave passing through the waveguide structure (=$\Re(\varepsilon_{\text{eff,h}})$) varies with frequency, being negative below the cut-off frequency, and positive above, and remains always lower than the dielectric constant ε_r of the filling composite that is the polymer composite material 30. On the contrary, the imaginary part is not modified with respect to the composite alone, meaning that the conductivity seen by the wave is not affected by the waveguide.

[0059] Canonical expressions for the propagation constant only exist for rectangular or circular geometries of the metallic grid panel 20. It is however possible to derive analytical expressions for any shape of waveguide by using perturbation techniques. For a hybrid material 10 including a metallic grid panel 20 with hexagonal holes (honeycomb lattice), one can obtain the following expression of the complex effective dielectric constant of the hybrid material:

$$\varepsilon_{\text{eff,h}} = \varepsilon_r - \left(1 + \frac{\cos\alpha}{1+2\cos\alpha}\right)\left[\left(\frac{m\pi}{a}\right)^2 + \left(\frac{n\pi}{b}\right)^2\right]\left(\frac{c_0}{w}\right)^2 - \frac{j\sigma}{\omega\varepsilon_0} \quad \text{(Eq. 9)}$$

with $a = (1 + 2\cos\alpha)X$ and $b = 2X\sin\alpha$, with X and α fixing the shape of the hexagonal holes (see figure 2(a)).

[0060] By using equations (Eq. 3) and (Eq. 9), one can calculate the absorption index *A* of sample 1 whose measured absorption index is shown in figure 3. Figure 5 shows the calculated variation of the real part of the complex effective dielectric constant of sample 1 with respect to frequency. From equation (Eq. 9), the cut-off frequency for which $\Re(\varepsilon_{\text{eff,h}}) = 0$ is around 6.3 GHz for sample 1. Above this frequency, the real part of the effective dielectric constant for the hybrid material 10 (solid line) remains lower than for the composite polymer material 30 alone (dashed line). As a consequence, the reflected power is reduced. This is confirmed in figure 6 that shows the measured reflection index $R = P_r/P_i$ in decibels for the hybrid material 10 (solid line) and for the polymer composite material 30 alone (dashed curve). Figure 4 shows the calculated absorption index *A* per unit thickness versus frequency with $\alpha = 60°$, $X = 6\,mm$, $\varepsilon_r = 5$, $m = 1$, and $n = 0$ (ε_r is the dielectric constant of the polymer composite material 30 filling the grid panel 20). The comparison between figure 3 and figure 4 shows a good agreement between the measurements and the calculations for the hybrid material 10 named sample 1. In particular, both the simulated and measured curves present a peak of the absorption index around the frequency 6.5 GHz. The differences between the measured and calculated curves can be attributed to experimental errors and to poor estimations of ε_r and σ entering equations (Eq. 3) and (Eq. 9).

[0061] As the thickness of the hybrid material 10 increases, higher values of the absorption index *A* can be obtained. Figure 7 shows the frequency evolution around 30 GHz of the calculated absorption indices of two materials when their thickness is equal to 3 cm. The solid curve corresponds to the hybrid material 10 of the invention (where we assume $t_1 = t_2$) whereas the dashed curve relates to the polymer composite material 30 alone. The electrical conductivity of the latter is assumed to be equal to 0.5 S/m whereas $\varepsilon_r = 3$. The grid panel 20 is assumed to be a metallic honeycomb lattice characterized by the parameter *X* = 2 mm (see figure2(a)). Once again, we observe in figure

7 that the absorption index *A* increases after the insertion of the grid panel 20 in the polymer composite material 30. We also observe that very high absorption indices can be obtained above the cut-off frequency of the grid panel 20 with the hybrid material 10: when f ~ 32 GHz, A ~ 99,17 % when one uses the hybrid material 10 with a thickness equal to 3 cm.

[0062] In the above examples, the thickness t_1 of the grid panel 20 is equal to the thickness t_2 of the polymer composite material 30. A sample having $t_2 < t_1$ and that we name sample 2 has been prepared by the same technique as sample 1. Sample 2 is a hybrid material 10 whose grid panel 20 is an aluminium honeycomb lattice of thickness $t_1 = 8$ mm characterized by a cell size X=7 mm (see figure 2(a)). The polymer composite material 30 that is a polyurethane foam charged with 2 wt% of CNT has a thickness $t_2 = 3$ mm and fills the holes 25 of the grid panel 20 along the thickness $t_2 = 3$ mm. Figure 8 shows the measured evolution of the absorption index *A* in percent with frequency for sample 2 (solid line) and for the polymer composite material 30 alone (dashed curve). As for sample 1, we observe that the insertion of the grid panel 20 allows one to increase the absorption capabilities. In figure 8, the increase is large: for f~8 GHz, the absorption index *A* increases from around 30 % for the polymer composite material 30 alone to around 90 % when the grid panel 20 is inserted.

[0063] The analytical results obtained by equations (Eq. 3) and (Eq. 9) were compared with results obtained by Finite-Element simulations. In the latter case, the Comsol software (http://www.comsol.com/) that solves Maxwell's equations was used. Two kinds of simulations were carried out: one series with a slab composed of only a polymer composite material 30, and another one with a slab comprising a metallic honeycomb grid panel 20 inserted in the polymer composite material 30. Figure 9 (a) shows the geometry used in the first series of simulations whereas figure 9 (b) shows the geometry used in the second case. From these figures, we see that the polymer composite material 30 and the metallic honeycomb grid panel 20 have the same thickness, which means $t_1 = t_2$. The slab is sandwiched between two thin air layers modeling the surrounding environment. The advantage of using analytical calculations and Finite-Element simulations is that the parameters characterizing the hybrid material 10 can be changed easily to study their effect on the absorbing power.

The following parameters were varied: the electrical conductivity σ of the polymer composite material 30, the thickness *t* of the slab, and the size *X* of the side of a hexagonal hole 25.

[0064] Figures 10 and 11 show the results of the analytical calculations and of the simulations for the variation of the absorption index *A* (in percent) with respect to frequency. In figure 10 (respectively figure 11), the electrical conductivity σ of the polymer composite material 30 is equal to 0.5 S/m (respectively 1 S/m). In both cases, the thickness of the slab is equal to t = 5 mm and the dielectric constant of the polymer composite material 30 is equal to $\varepsilon_r = 3$. First, we observe a very good agreement between the variation of the absorption index calculated analytically (continuous, dashed, and dash-dotted curves) and by the simulations (triangles, squares, circles). Both in figures 10 and 11, we observe that above a given frequency, the absorption index *A* is increased when the metallic honeycomb grid panel 20 is inserted in the polymer composite material 30. As expected, when the electrical conductivity of the polymer composite material 30 increases, the absorption index also increases. When the size *X* of the side of a honeycomb hole is decreased (from 2 mm to 0.9 mm), the frequency for which the absorption presents a peak is increased (from f ~ 30 GHz to f ~ 60 GHz). This is due to the increase of the cut-off frequency of the metallic grid as *X* decreases. Hence, an additional advantage of the hybrid material 10 of the invention is to allow one to change the frequency range corresponding to a high power absorption by modifying the size of the holes 25 of the grid panel 20. A peak in the absorption index results in a lower reflection index $R = P_r/P_i$. This is illustrated in figure 12 which shows the calculated reflection index $R = P_r/P_i$ (in decibels) versus frequency for the hybrid material 10 when *X*=0.9 mm, $\varepsilon_r = 3$, t = 5 mm, and $\sigma = 0.5\,S/m$ (solid curve). The dashed curve represents the frequency variation of the reflection index for the polymer composite material 30 alone. By comparing figure 12 with figure 10 (dashed curve and square symbols), we observe that the reflection index is minimum in the frequency range where the absorption index is maximum.

[0065] Figure 13 shows the results of the analytical calculations and of the simulations for the variation of the absorption index (in percent) with respect

to frequency when the thickness of the slab t (see figures 9(a) and 9(b)) is increased to t = 10 mm. As in figure 10, the electrical conductivity of the polymer composite material 30 is equal to 0.5 S/m, and its dielectric constant is equal to $\varepsilon_r = 3$. As expected, by comparing figure 10 and figure 13, we observe that the power of absorption of the hybrid material 10 is increased when the thickness t is increased.

[0066] By modifying the size of the holes of the grid panel 20, one can change the frequency corresponding to the strongest absorption of the hybrid material 10. Another possibility to modulate the frequency for which a peak of maximum absorption is observed is to deform the hybrid material 10 and hence the grid panel 20. This is illustrated in figure 14 where a hybrid material of thickness t = 5 mm, with a polymer composite material 30 of conductivity $\sigma = 1\,S/m$ and dielectric constant $\varepsilon_r = 3$ is used. This figure shows a comparison of the evolution of the absorption index with frequency when the grid panel 20 is a metallic regular honeycomb lattice ($\alpha = 60°$) or a deformed one ($\alpha = 18°$). As a reminder, figure 2(a) shows how α is defined and it is assumed in these calculations that the thickness t_1 of the grid panel 20 is equal to the thickness t_2 of the polymer composite material 30. From figure 14, we see that the frequency corresponding to a peak of the index A decreases as α decreases. Hence, the variation of the angle α is another possibility to modulate the peak of maximum absorption of the hybrid material 10.

[0067] Compared to a single polymer composite material 30, the hybrid material 10 introduces additional degrees of freedom towards multifunctional panels, with a potential to optimize density, stiffness, and thermal insulation. In order to show the potential of the new hybrid material 10, two material selection procedures involving an electromagnetic absorption constraint and an objective towards optimizing another material property are described now, following the rationale developed by M. F. Ashby in “Materials Selection in Mechanical Design, Third edition” (Elsevier 2005).

[0068] A first important design constraint typical of transportation or human body protection (e.g. helmet) is lightness. Assuming that the thickness of an absorbing slab is a free constant, the performance index M_1 for a light electromagnetic absorption panel is given by:

$$M_1 = 1/(\rho\, t) \quad \text{(Eq.10)}$$

where ρ and t are respectively the relative density (with respect to the water density) of the used material and the thickness of the slab. Imposing a level of the absorption index *A* of equation (Eq. 2), the performance index M_1 can be calculated by using equations (Eq. 3) and equation (Eq. 10) for different materials for which ρ, ε_r and σ are known. Figure 15 shows at several frequencies the value of the performance index M_1 for different materials for which the absorption index *A* has been fixed to 90 %. These materials are leather, plaster of Paris, SiC foam, a nanocomposite foam being a 2 wt%-CNT reinforced polyurethane foam (polymer composite material 30) and two hybrid materials 10 comprising such a reinforced polyurethane foam for the polymer composite material 30 and a grid panel 20 being an aluminium regular honeycomb lattice (for the two hybrid materials, we assume that $t_1 = t_2$). The hybrid material named hybrid 1 is characterized by the parameter *X*=4.7 mm whereas the hybrid material named hybrid 2 has *X*=1.58 mm. The nanocomposite foam has a dielectric constant ranging between 3 and 3.5, an electrical conductivity ranging between 0.7 and 1.2 S/m, and a relative density of 0.3. Hybrid 1 (respectively hybrid 2) has a relative density of 0.39 (respectively 0.44).

[0069] The SiC foam has a low performance index (M_1=2) for all the frequencies and is not visible in figure 15. The plaster of Paris does not reach an absorption level of 0.9 with as consequence that M_1 is equal to zero. Leather could theoretically compete with the nanocomposite foam at 10 GHz. Above this frequency, the latter is significantly better. The hybrid materials 10 of the invention perform extremely well when a high absorption is desired (*A*=0.9), not only because of the high electromagnetic absorption capacity which is better than any other material, but owing also to the lightness of the association of the foam polymer composite material 30 and the grid panel 20. Their outstanding performances are determined in a desired frequency range function of the honeycomb hole dimension (e.g. 10-20 GHz for Hybrid 1 and 30-50 GHz for Hybrid 2). Even lighter hybrid materials 10 could be obtained with a metalized polymer based grid panel 20. For protection and mechanical strength in bending, face sheets can be added on one or on the two sides of the hybrid

material 10. It can be noted that the corresponding thickness relative to the hybrid materials are realistic for applications (between 5 and 15 mm).

[0070] The second selection procedure aims at finding the optimum material for an application involving electromagnetic absorption and thermal dissipation. This is typical of an electric or electronic device from which heat must be evacuated. Here, we assume that the grid panel 20 is an aluminium honeycomb lattice. The performance index M_2 for a slab with maximum thermal conductivity at a given absorption level is given by

$$M_2 = \lambda / t \qquad \text{(Eq. 11)}$$

where λ is the thermal conductivity of the slab. The performance indices M_2 of the six materials used in the first selection procedure were calculated and compared. As above, the absorption index A has been fixed to 90 %. The thermal conductivity can be predicted from a simple multi-steps homogenization theory starting from the CNT reinforced polymer up to the hybrid material 10. The key point, confirmed by experimental measurements, is that the presence of CNT leads to only a very limited enhancement of the thermal conductivity. Hence, a lower bound homogenization model can be used. The thermal conductivity of the hybrid material 10 essentially comes from the aluminium grid panel 20 for which a minimum value of 100 W/(m K) was chosen for the thermal conductivity. Figure 16 presents the evolution of the performance indices M_2 versus frequency for the six studied materials. The evolution of the index M_2 of the plaster of Paris is too low to be visible on figure 16. From this figure, we see that once again the hybrid materials 10 show very interesting properties. Leather and SiC foam could compete with the nanocomposite foam but are far to reach the performance of hybrid 1 over the whole frequency range and hybrid 2 from 30 GHz. The nanocomposite foam has a thermal conductivity evaluated to $\lambda = 0.067\ \mathrm{W/(m\,K)}$, the hybrid 1 presents $\lambda = 4.13\ \mathrm{W/(m\,K)}$, whereas the thermal conductivity of the hybrid 2 is around $\lambda = 11.56\ \mathrm{W/(m\,K)}$. In order to ensure good thermal conductivity, one face metallic sheet could be added (on the outer surface, to avoid reflectivity). On the opposite, in applications requiring good thermal insulation, the metallic grid panel 20 can be replaced by a polymer grid panel 20 such that the internal surface of its holes 25 is metalized.

[0071] Other properties such the bending stiffness or strength of the hybrid material 10 can be optimized by addition and proper selection of face sheet materials. Additional degrees of freedom are provided by using graded foam densities for the polymer composite material 30 and more complex hole shapes. To widen the frequency range where the hybrid material 10 presents a large absorption index, one could use a superposition of grid panels 20 filled with eventually different polymer composite materials 30, each grid panel 20 having a different hole size. Hence, the hybrid material 10 can include more than one grid panel 20 and more than one polymer composite material 30.

[0072] As stated above, one possibility to decrease the frequency corresponding to a high power of absorption of the hybrid material 10 is to increase the size of the holes 25 of the grid panel 20. Then, one also has to increase the thickness *t* of the hybrid material 10 to keep high levels of absorption. However, such an increase cannot be too large except for anechoic chambers and other building applications. To overcome this problem, the inventors propose to superpose different hybrid materials 10 separated by dielectric layers 80. To obtain such a material, one can simply glue the different layers (hybrid material 10 and dielectric layer 80) by using all known gluing techniques.

[0073] The hybrid material 10 can be represented by the equivalent circuit of figure 17. The inductance L_2 and the capacitance C_2 of figure 17 form a resonant circuit characterized by a cut-off frequency. Below this frequency, there is no transmission and total reflection because L_2 dominates over C_2, forming the circuit $\{L_1,L_2\}$. Above the cut-off frequency of the hybrid material 10, there is transmission with attenuation following the transmission characteristics of the circuit composed of $\{L_1,C_2\}$. If now, a dielectric layer 80 composed of a polymer composite material 30 as an example is inserted between two layers of hybrid material 10, the resultant equivalent circuit is the one depicted in figure 18. We see that the capacitance C_1 has been added: the two hybrid materials 10 form the electrodes of a capacitor and the dielectric layer 80 is the dielectric between these two electrodes. Hence, the equivalent circuit of the resultant material includes two resonant circuits $\{L_1,C_1\}$ and $\{L_2,C_2\}$. From this circuit, we deduce that transmission (with absorption) is possible when L_1 dominates over C_1 and C_2 dominates over L_2 (circuit $\{L_1,C_2\}$) or when C_1 dominates over L_1 and

L_2 dominates over C_2 (circuit $\{C_1,L_2\}$). Transmission with circuit $\{C_1,L_2\}$ is not classical and is called « left-handed », because the group and phase velocities of the transmitted signal are in opposite direction. More than two hybrid materials 10 can be used, each separated by a dielectric layer 80 in order to get a quasi-homogeneous structure with respect to the wavelength in the direction of propagation.

[0074] Figure 19 shows the calculated absorption index versus frequency carried out by a hybrid material 10 (dashed curve) and by a material comprising fifteen hybrid materials 10, each separated by a dielectric layer 80 (solid curve). The used grid panel 20 is an aluminium honeycomb lattice with a hole size *X* equal to 1 cm. The dielectric layers 80 are assumed to be composed of the same material as the composite polymer material 30 filling the different grids. This material is assumed to have a dielectric constant equal to $\varepsilon_r = 3$ and an electrical conductivity equal to 0.1 S/m. Each hybrid material 10 has a thickness equal to 1 mm, whereas the thickness of the dielectric layers 80 between each hybrid material 10 is equal to 0.25 mm. The hybrid material 10 corresponding to the dashed curve of figure 19 has a thickness equal to 15*1 mm = 1,5 cm. For all hybrid materials 10, we assume $t_1 = t_2$. We see in figure 19 that the absorption index *A* of the material composed of the fifteen hybrid materials 10 separated by dielectric layers 80 is larger than the absorption index *A* of the hybrid material 10 alone at low frequency. Such a combination of hybrid materials can thus be used to absorb electromagnetic waves at lower frequencies while keeping reasonable overall thickness.

[0075] The measured and calculated performances of the hybrid material 10 and of the material including two or more hybrid materials 10 separated by dielectric layers 80 according to the invention show that efficient power of electromagnetic absorption can be obtained in the form of light stiff panels, said panels eventually forming a closed enclosure, with thermal management coming from the choice of the grid panel 20 and the polymer composite material 30, opening to many applications requiring electromagnetic absorption in housing, electronics, health protection as well as electromagnetic active filtering by changing the dimensions of the grid panel 20. At some frequencies, the absorption index increases from 30 % for a polymer composite material 30 alone to around 90 % for a hybrid material 10 according to the invention. The

invention also relates to the use of a hybrid material 10 or the use of two or more hybrid materials 10 separated by dielectric layers 80 for absorbing an electromagnetic radiation.

[0076] The terms and descriptions used herein are set forth by way of illustration only and are not meant as limitations. Those skilled in the art will recognize that many variations are possible within the spirit and scope of the invention as defined in the following claims, and their equivalents, in which all terms are to be understood in their broadest possible sense unless otherwise indicated. As a consequence, all modifications and alterations will occur to others upon reading and understanding the previous description of the invention. In particular, dimensions such the parameters X, t_1, t_2 and α of figure 2(a), materials, stacking sequence of hybrid materials 10, and other parameters given in the above description may vary depending on the needs of the application.

CLAIMS

1. A hybrid material (10) for absorbing electromagnetic radiation (60) comprising
at least one grid panel (20) of thickness t_1 having holes (25) traversing said thickness t_1,
at least one polymer composite material (30) of thickness t_2 filling at least partially the holes (25) of the at least one grid panel (20), said at least one polymer composite material (30) including a polymer matrix (40) and conductive particles (50) dispersed into said polymer matrix (40),
characterized in that
the internal surface of the holes (25) of the at least one grid panel (20) is metallic.

2. Hybrid material (10) according to claim 1 characterized in that the thickness t_2 of the at least one polymer composite material (30) filling at least partially the holes (25) of the at least one grid panel (20) is smaller than the thickness t_1 of said at least one grid panel (20).

3. Hybrid material (10) according to any of the previous claims characterized in that the shape of the holes (25) traversing the thickness t_1 of the grid panel (20) is a prism with a hexagonal base.

4. Hybrid material (10) according to any of the previous claims characterized in that the conductive particles (50) dispersed into the polymer matrix (40) of the at least one polymer composite material (30) are carbon based conductive loads.

5. Hybrid material (10) according to claim 4 characterized in that the carbon based conductive loads comprise carbon based fillers, carbon nanotubes, carbon black or a mixture thereof.

6. Hybrid material (10) according to claim 4 characterized in that the carbon based conductive loads are carbon nanotubes positioned in such a manner that their axes are perpendicular to the thickness t_1 of the at least one grid panel (20).

7. Hybrid material (10) according to any of the previous claims characterized in that the at least one grid panel (20) is metallic.

8. Hybrid material (10) according to any of claims 1 to 6 characterized in that the at least one grid panel (20) is not metallic and in that the internal surface of the holes (25) of the grid panel (20) is metalized.

9. Hybrid material (10) according to any of the previous claims characterized in that the lateral surfaces of the hybrid material (10) are covered by additional sheets of materials whereby the bending stiffness and / or the mechanical strength of the resultant panel are increased.

10. Hybrid material (10) according to any of the previous claims characterized in that the holes (25) size of the grid panel (20) is tailored in order to improve the absorption of an incident electromagnetic radiation (60) in a range of frequency.

11. Hybrid material (10) according to any of the previous claims characterized in that the hybrid material (10) is deformed in order to improve the absorption of an incident electromagnetic radiation (60) in a range of frequency.

12. Hybrid material (10) according to any of the previous claims characterized in that the at least one polymer composite material (30) is a foam.

13. Hybrid material (10) according to claim 12 characterized in that the foam presents a gradient of foam density.

14. Hybrid material (10) according to any of the previous claims further comprising at least one dielectric layer (80) between said hybrid material (10) and at least one additional hybrid material (10).

15. Material according to claim 14 characterized in that the dielectric layer (90) comprises a polymer matrix (40).

16. Process for making a hybrid material (10) according to any of the previous claims including the steps of :

a) forming a polymer composite material (30) by dispersion of particles in a melt polymer matrix (40) or by a co precipitation process,
b) inserting a grid panel (20) of thickness t_1 having holes (25) traversing said thickness t_1 in the polymer composite material (30),
c) optionally foaming the polymer composite material (30) before or after step b).

17. Process for making a hybrid material (10) according to any of the previous claims including the steps of :

i. casting in a grid panel (20) of thickness t_1 having holes (25) traversing said thickness t_1 reactants that are monomers, solvent, particles, catalyst or polymerization initiator,
ii. exposing the set obtained in step i to polymerization conditions,
iii. optionally foaming the resultant material.

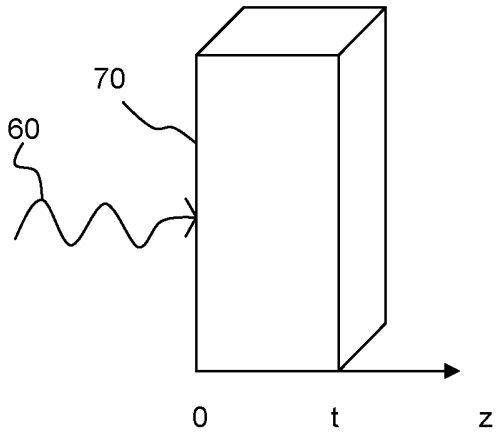

Fig. 1

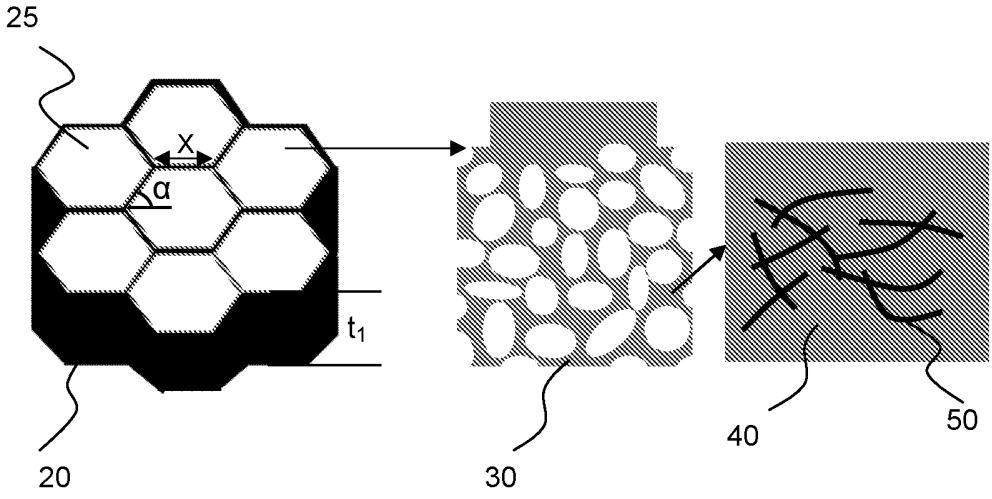

Fig. 2

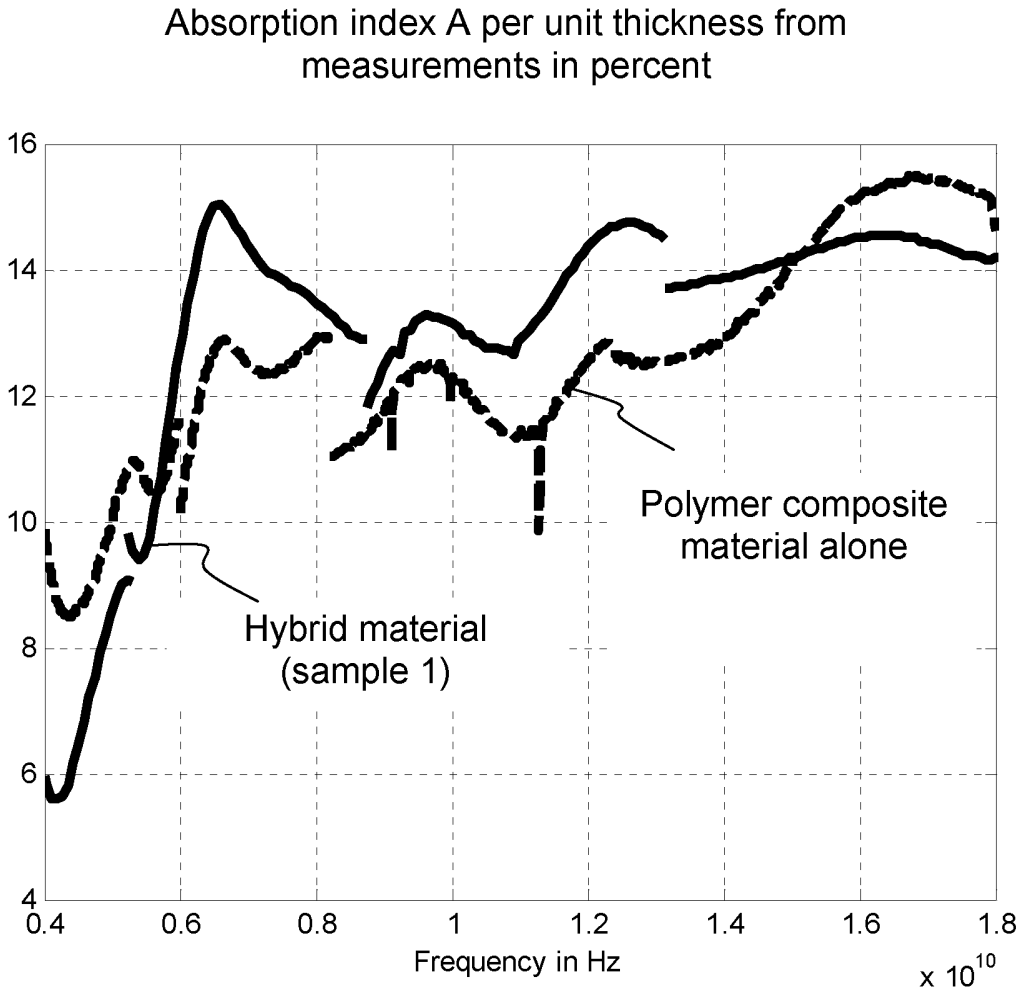
Absorption index A per unit thickness from measurements in percent
16
14
12
10
8
6
4
0.4
0.6
0.8
1
1.2
1.4
1.6
1.8
Frequency in Hz
x 10^10
Polymer composite material alone
Hybrid material (sample 1)

Fig. 3

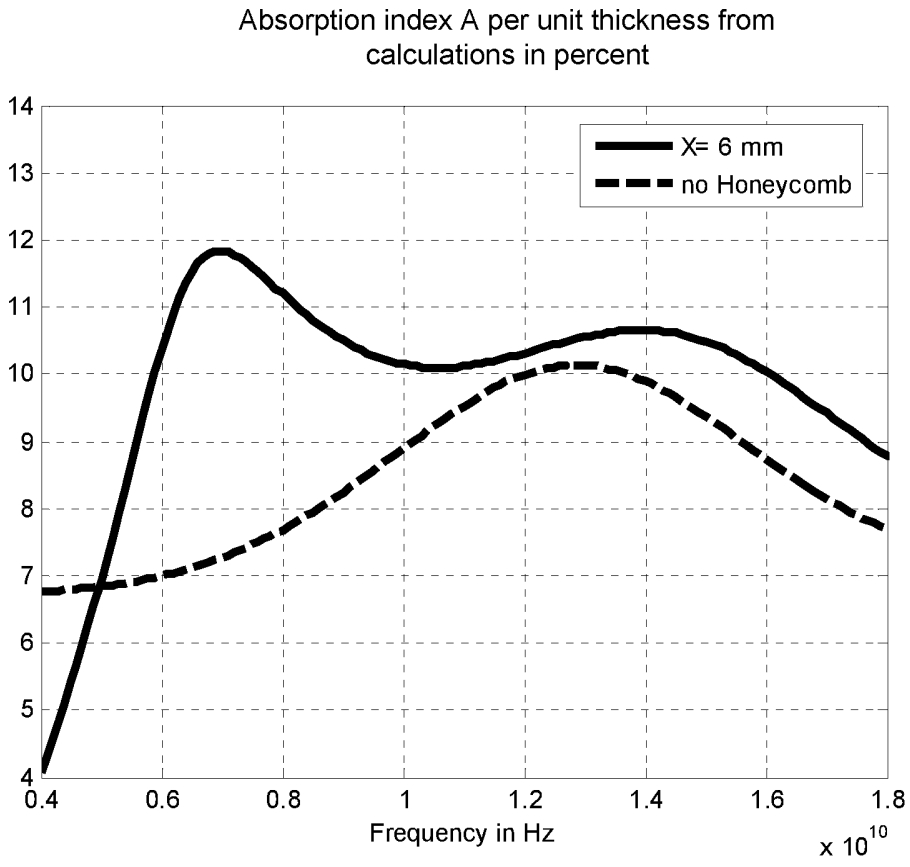
Absorption index A per unit thickness from calculations in percent
X= 6 mm
no Honeycomb
14
13
12
11
10
9
8
7
6
5
4
0.4
0.6
0.8
1
1.2
1.4
1.6
1.8
Frequency in Hz
x 10^10

Fig. 4

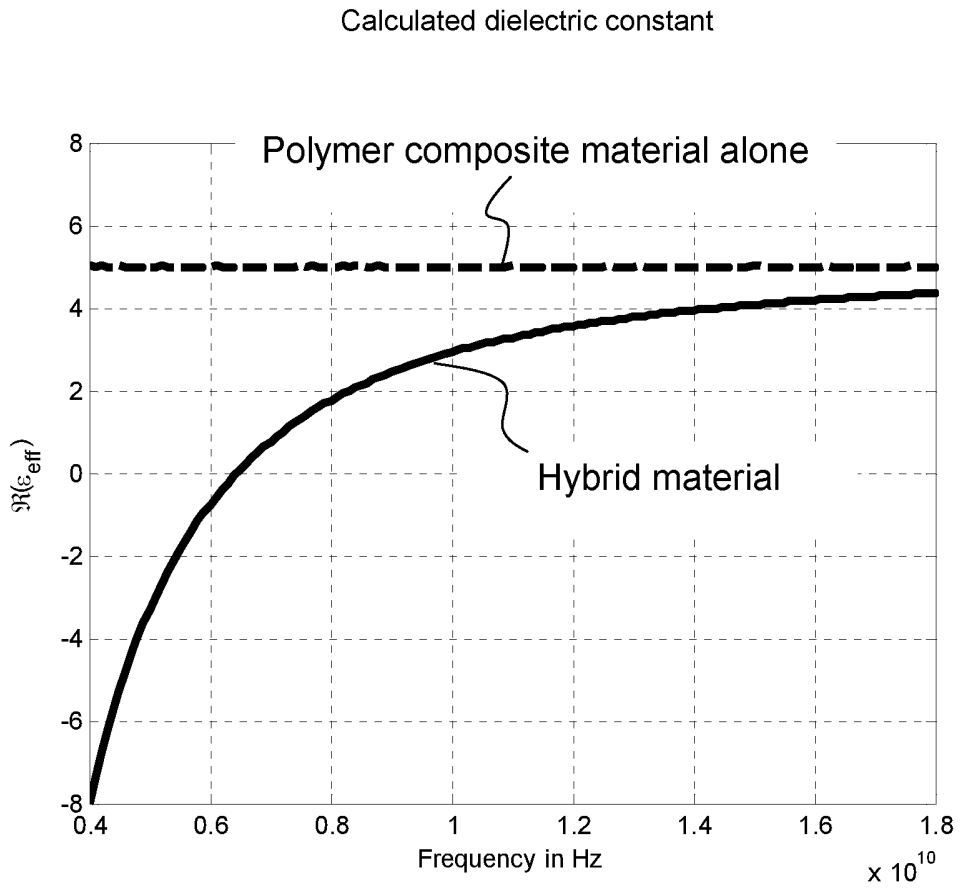
Calculated dielectric constant
Polymer composite material alone
Hybrid material
$\Re(\varepsilon_{eff})$
8
6
4
2
0
-2
-4
-6
-8
0.4
0.6
0.8
1
1.2
1.4
1.6
1.8
Frequency in Hz
x 10^{10}

Fig. 5

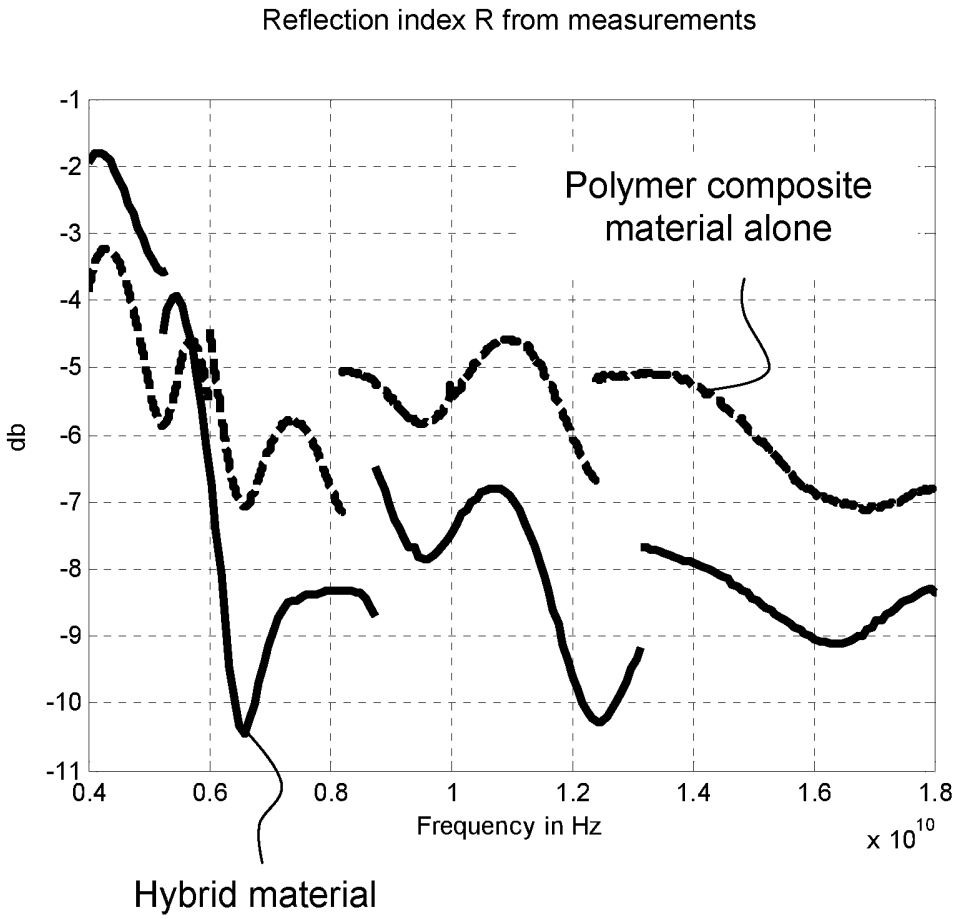
Reflection index R from measurements
Polymer composite material alone
Hybrid material
db
-1
-2
-3
-4
-5
-6
-7
-8
-9
-10
-11
0.4
0.6
0.8
1
1.2
1.4
1.6
1.8
Frequency in Hz
x 10^10

Fig. 6

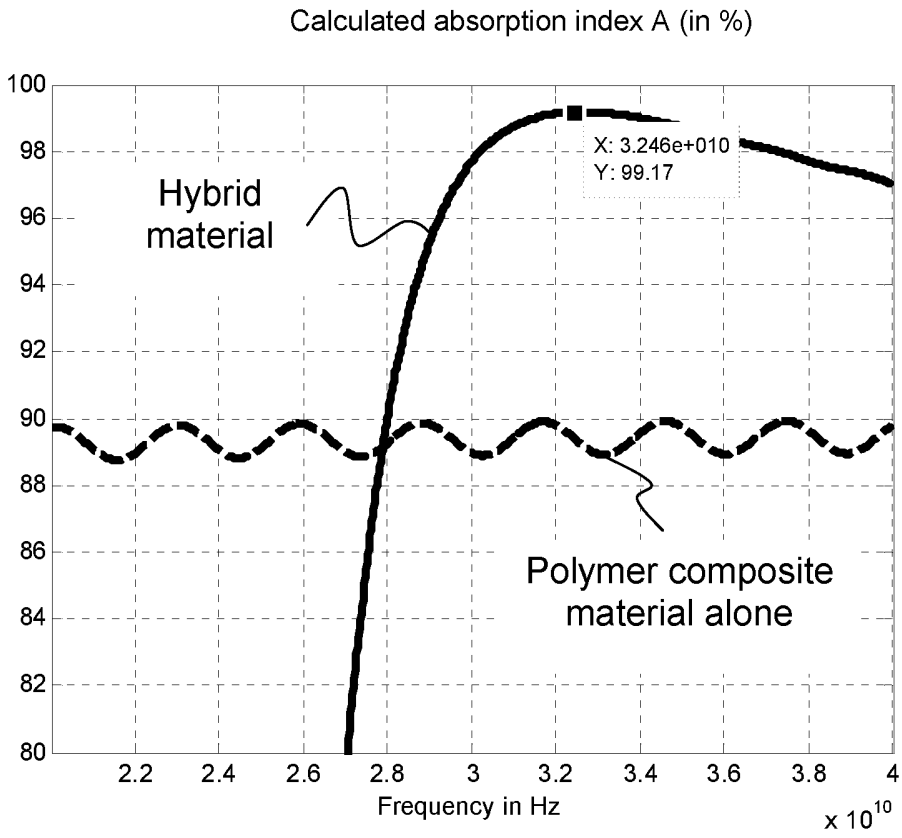
Calculated absorption index A (in %)
100
98
96
94
92
90
88
86
84
82
80
2.2
2.4
2.6
2.8
3
3.2
3.4
3.6
3.8
4
Frequency in Hz
x 10^10
X: 3.246e+010
Y: 99.17
Hybrid material
Polymer composite material alone

Fig. 7

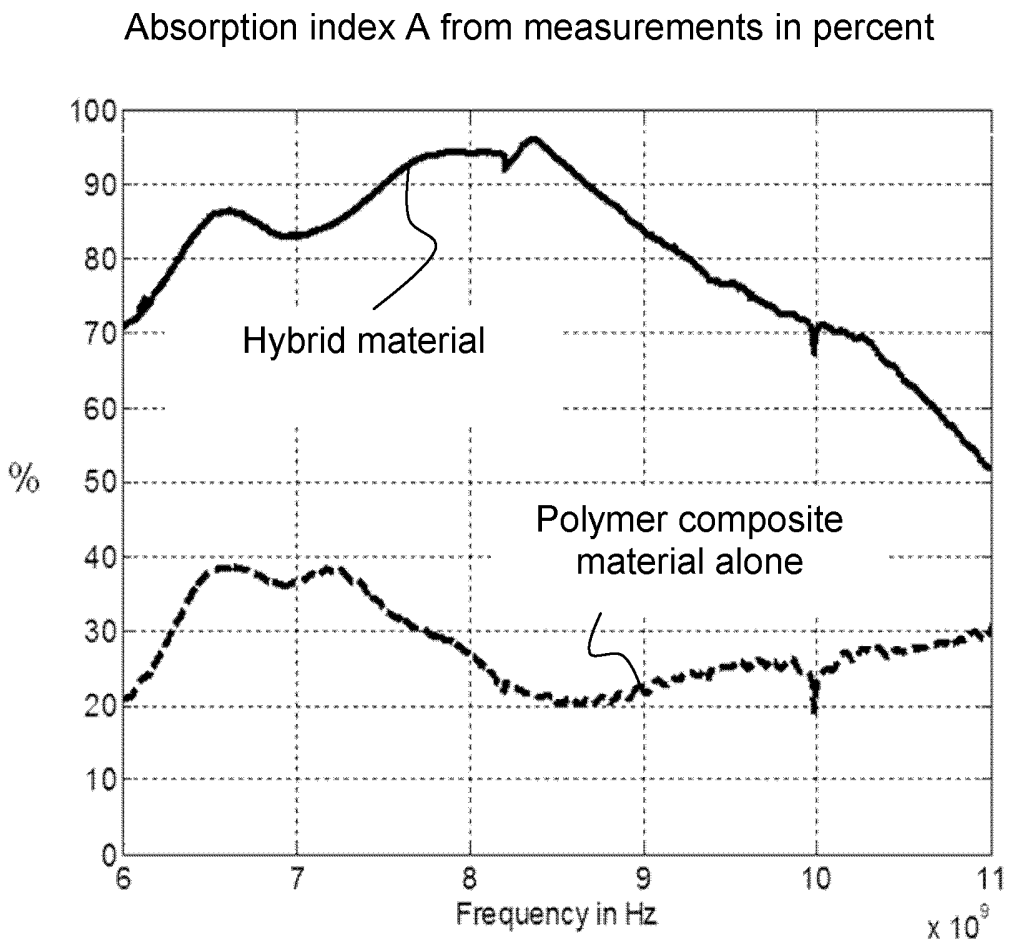
Absorption index A from measurements in percent
100
90
80
70
60
50
40
30
20
10
0
%
Hybrid material
Polymer composite material alone
6
7
8
9
10
11
Frequency in Hz
x 10^9

Fig. 8

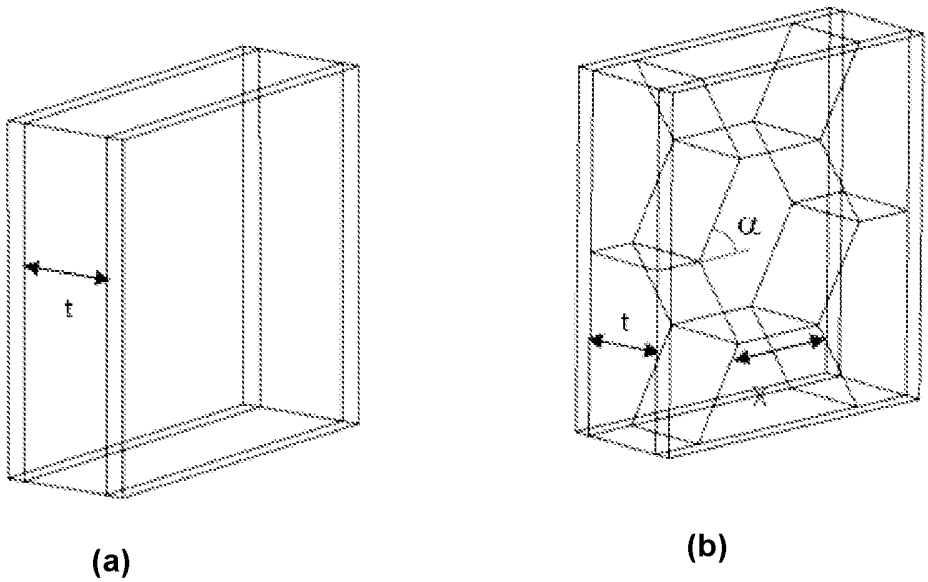
t
α
t
X
(a)
(b)

Fig. 9

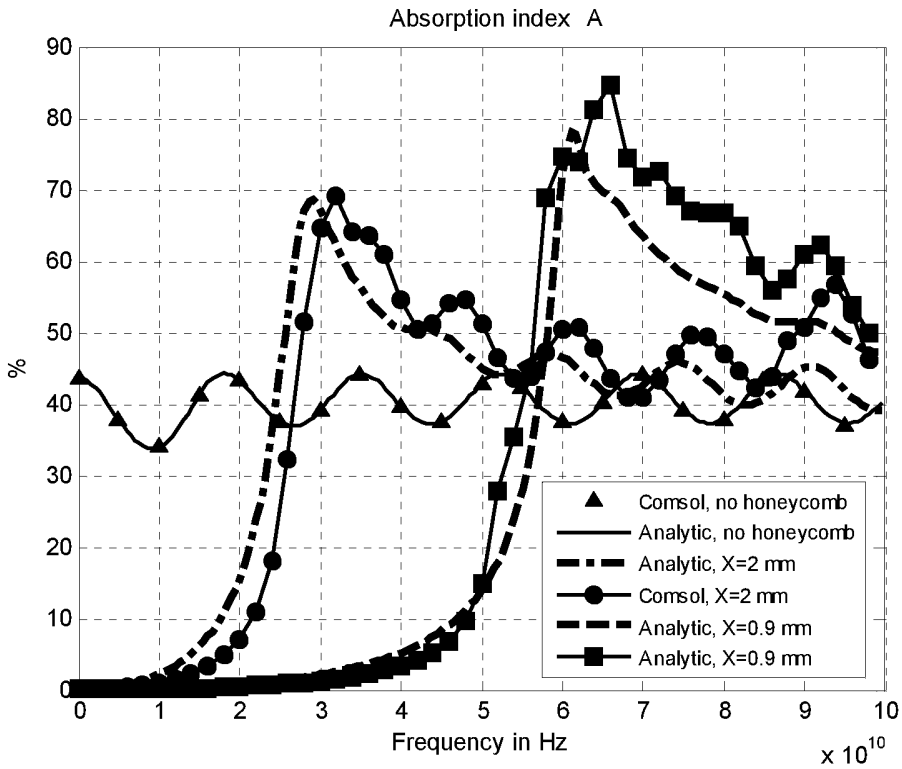
Absorption index A
%
Frequency in Hz
x 10^10
Comsol, no honeycomb
Analytic, no honeycomb
Analytic, X=2 mm
Comsol, X=2 mm
Analytic, X=0.9 mm
Analytic, X=0.9 mm

Fig. 10

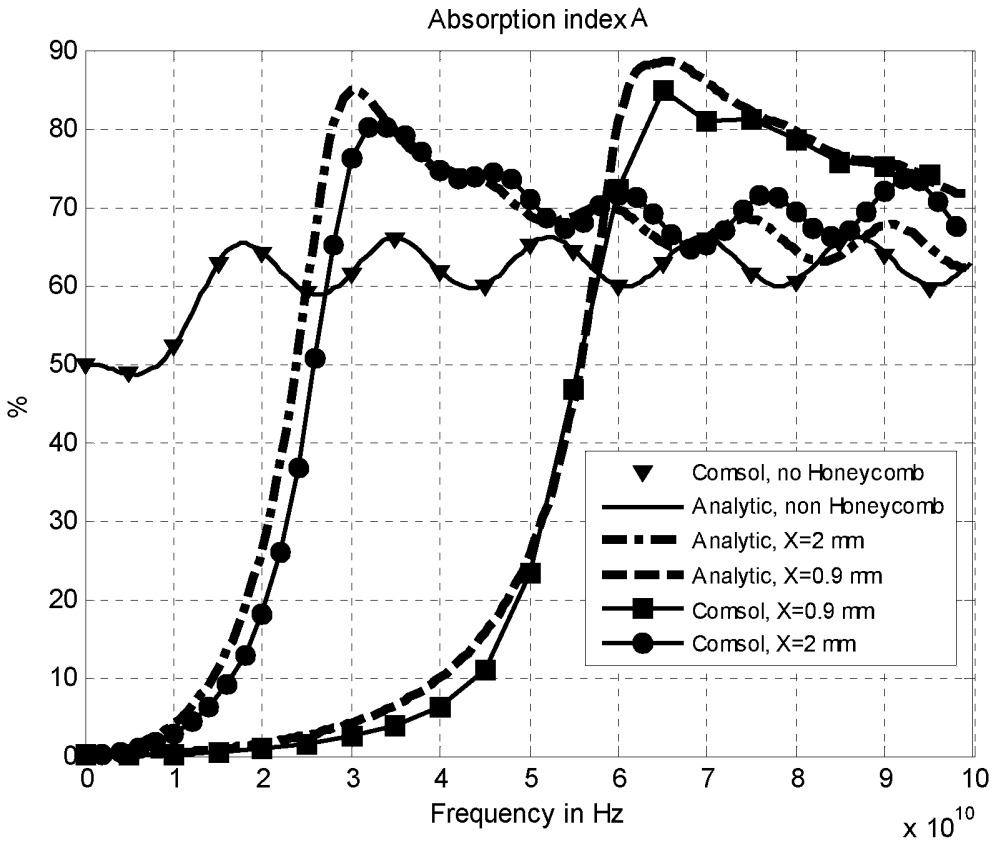
Absorption index A
90
80
70
60
50
40
30
20
10
0
%
0
1
2
3
4
5
6
7
8
9
10
Frequency in Hz
x 10^10
Comsol, no Honeycomb
Analytic, non Honeycomb
Analytic, X=2 mm
Analytic, X=0.9 mm
Comsol, X=0.9 mm
Comsol, X=2 mm

Fig. 11

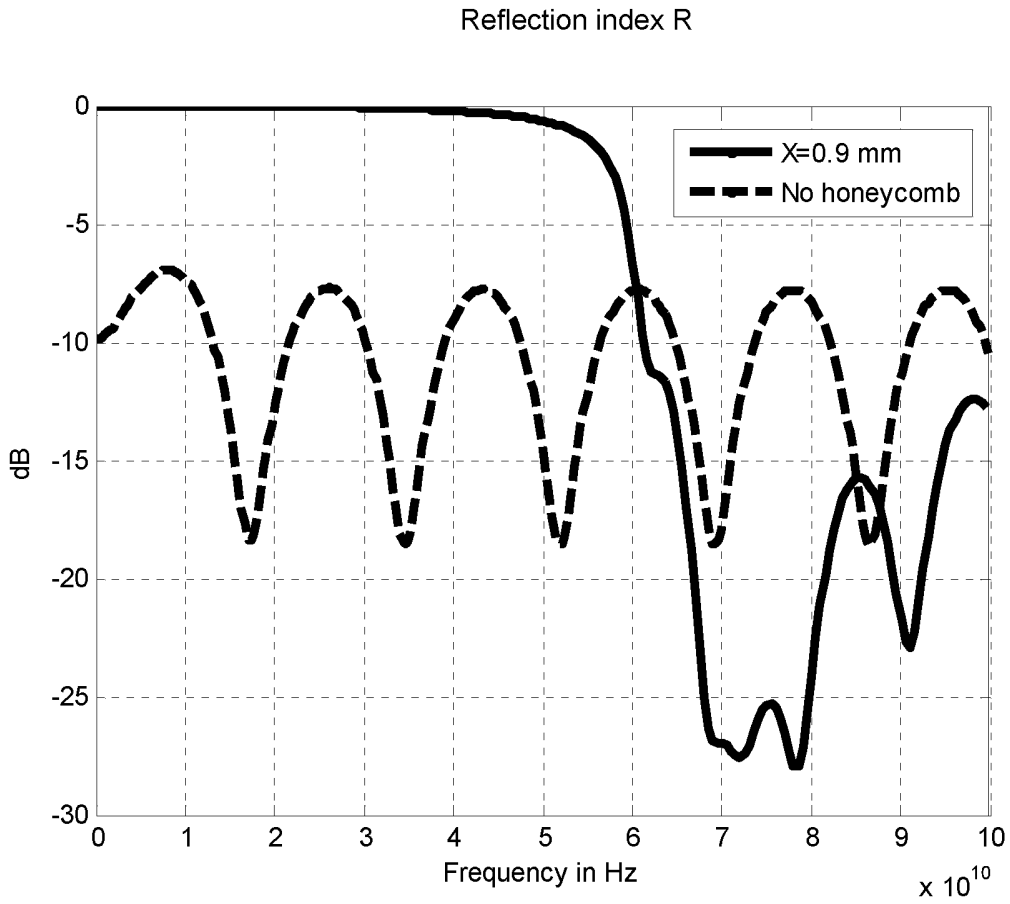
Reflection index R
X=0.9 mm
No honeycomb
dB
0
-5
-10
-15
-20
-25
-30
0
1
2
3
4
5
6
7
8
9
10
Frequency in Hz
x 10^10

Fig. 12

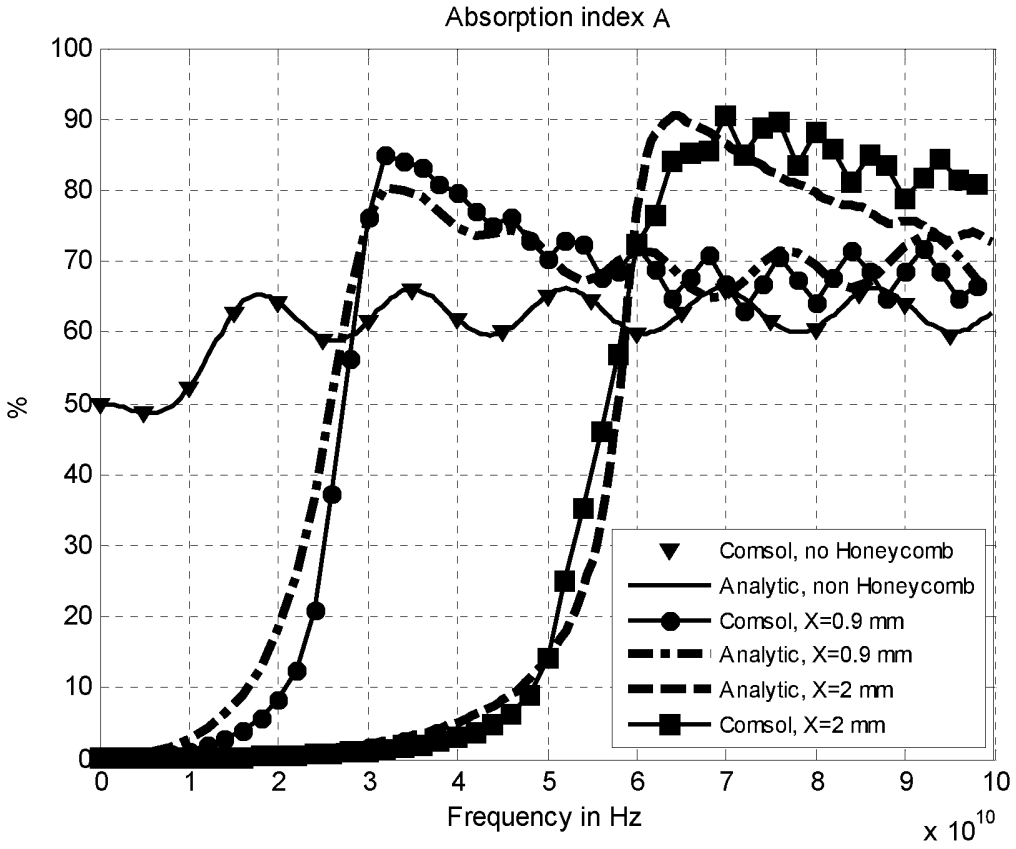
Absorption index A
100
90
80
70
60
50
40
30
20
10
0
%
0
1
2
3
4
5
6
7
8
9
10
Frequency in Hz
x 10^10
Comsol, no Honeycomb
Analytic, non Honeycomb
Comsol, X=0.9 mm
Analytic, X=0.9 mm
Analytic, X=2 mm
Comsol, X=2 mm

Fig. 13

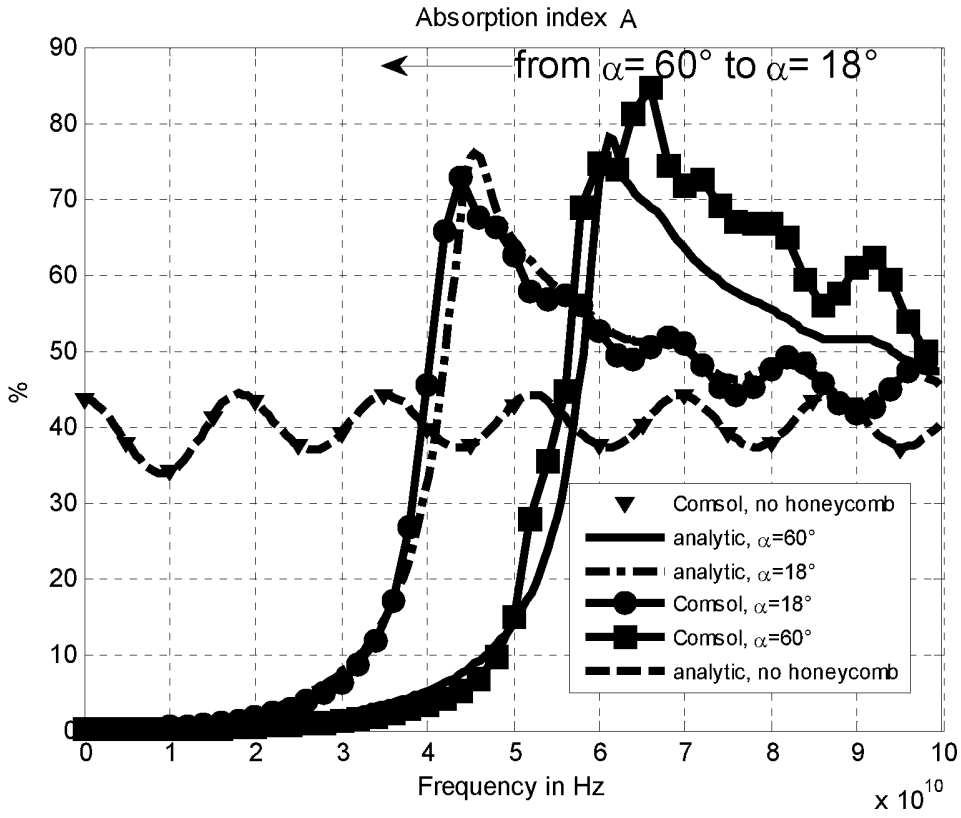
Absorption index A
from α= 60° to α= 18°
%
Frequency in Hz
x 10^10
Comsol, no honeycomb
analytic, α=60°
analytic, α=18°
Comsol, α=18°
Comsol, α=60°
analytic, no honeycomb

Fig. 14

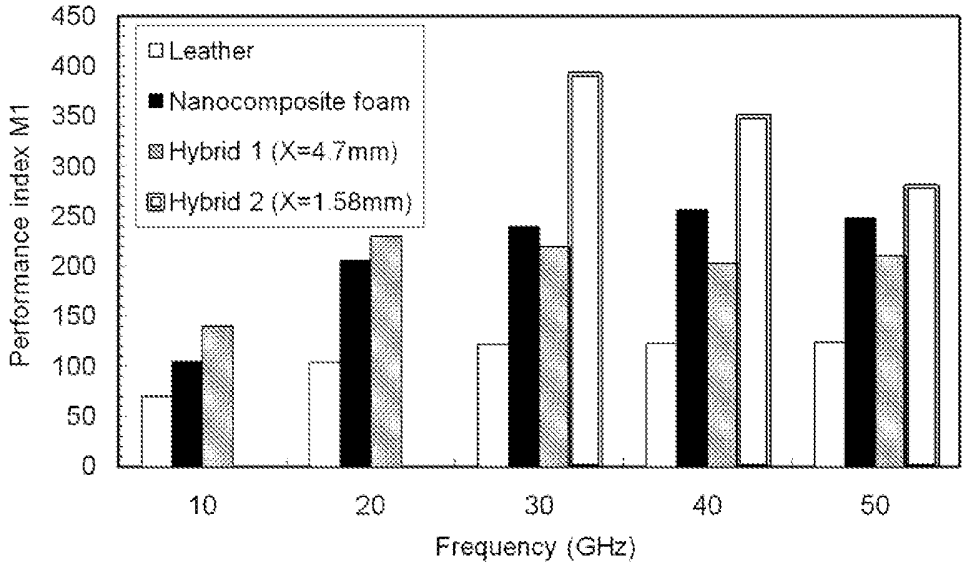
Performance index M1
450
400
350
300
250
200
150
100
50
0
Leather
Nanocomposite foam
Hybrid 1 (X=4.7mm)
Hybrid 2 (X=1.58mm)
10
20
30
40
50
Frequency (GHz)

Fig. 15

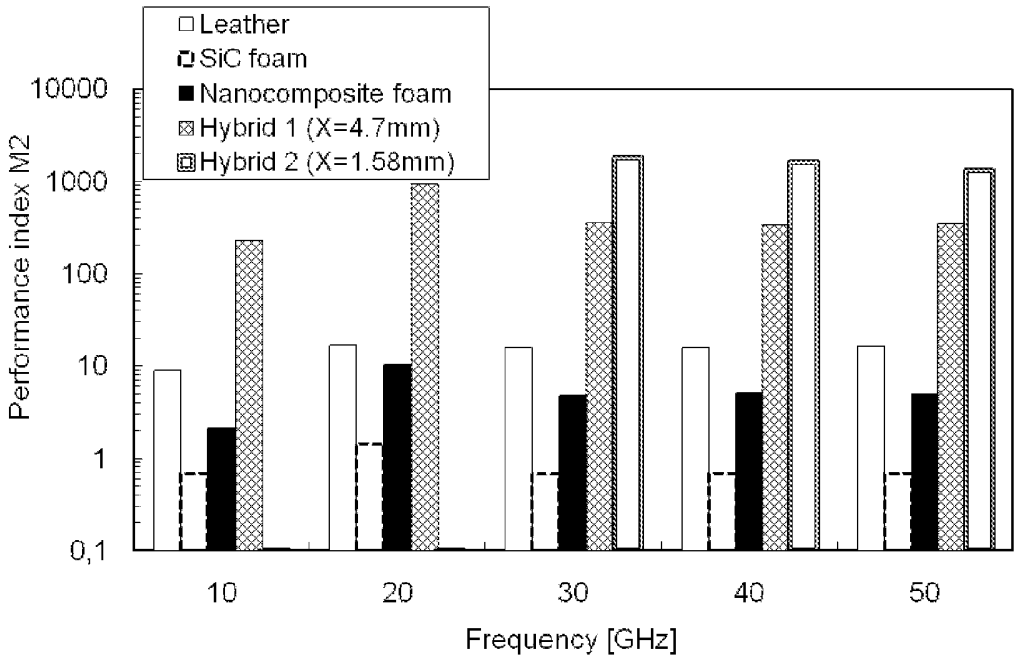
Leather
SiC foam
Nanocomposite foam
Hybrid 1 (X=4.7mm)
Hybrid 2 (X=1.58mm)
Performance index M2
10000
1000
100
10
1
0,1
10
20
30
40
50
Frequency [GHz]

Fig. 16

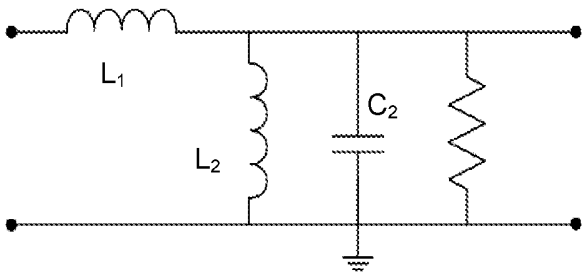
L1
L2
C2

Fig. 17

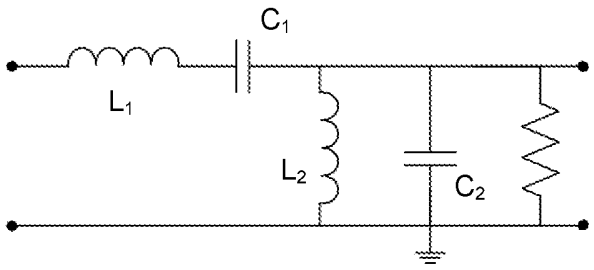

Fig. 18

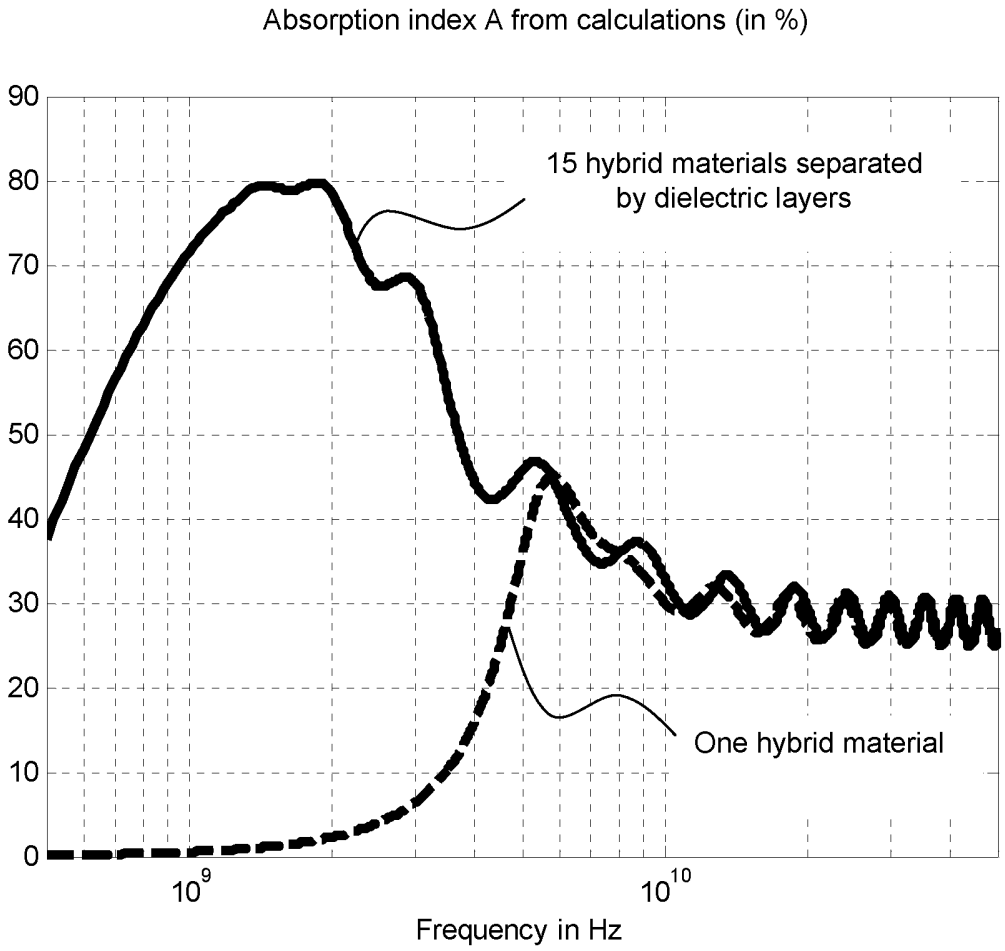
Absorption index A from calculations (in %)
90
80
70
60
50
40
30
20
10
0
15 hybrid materials separated by dielectric layers
One hybrid material
10^9
10^10
Frequency in Hz

Fig. 19

INTERNATIONAL SEARCH REPORT

International application No
PCT/EP2011/065554

A. CLASSIFICATION OF SUBJECT MATTER
INV. H01Q15/00 H01Q17/00
ADD.

According to International Patent Classification (IPC) or to both national classification and IPC

B. FIELDS SEARCHED

Minimum documentation searched (classification system followed by classification symbols)
H01Q

Documentation searched other than minimum documentation to the extent that such documents are included in the fields searched

Electronic data base consulted during the international search (name of data base and, where practical, search terms used)
EPO-Internal

C. DOCUMENTS CONSIDERED TO BE RELEVANT

Category*	Citation of document, with indication, where appropriate, of the relevant passages	Relevant to claim No.
A	US 2004/104836 A1 (MUKASA KOICHI [JP] ET AL) 3 June 2004 (2004-06-03) abstract; figure 2	1-17
A	GB 2 264 589 A (THOMSON CSF [FR]) 1 September 1993 (1993-09-01) abstract; figure 2 page 6, lines 1-30	1-17

☐ Further documents are listed in the continuation of Box C.

☒ See patent family annex.

* Special categories of cited documents :

"A" document defining the general state of the art which is not considered to be of particular relevance

"E" earlier document but published on or after the international filing date

"L" document which may throw doubts on priority claim(s) or which is cited to establish the publication date of another citation or other special reason (as specified)

"O" document referring to an oral disclosure, use, exhibition or other means

"P" document published prior to the international filing date but later than the priority date claimed

"T" later document published after the international filing date or priority date and not in conflict with the application but cited to understand the principle or theory underlying the invention

"X" document of particular relevance; the claimed invention cannot be considered novel or cannot be considered to involve an inventive step when the document is taken alone

"Y" document of particular relevance; the claimed invention cannot be considered to involve an inventive step when the document is combined with one or more other such documents, such combination being obvious to a person skilled in the art.

"&" document member of the same patent family

Date of the actual completion of the international search	Date of mailing of the international search report
5 October 2011	13/10/2011

Name and mailing address of the ISA/	Authorized officer
European Patent Office, P.B. 5818 Patentlaan 2 NL - 2280 HV Rijswijk Tel. (+31-70) 340-2040, Fax: (+31-70) 340-3016	Cordeiro, J

1

INTERNATIONAL SEARCH REPORT

Information on patent family members

International application No
PCT/EP2011/065554

Patent document cited in search report	Publication date	Patent family member(s)	Publication date
US 2004104836 A1	03-06-2004	AU 2003204967 A1	05-02-2004
		CA 2432970 A1	18-01-2004
		CN 1473004 A	04-02-2004
		DE 60305388 T2	29-03-2007
		DK 1383138 T3	02-10-2006
		EP 1383138 A1	21-01-2004
		HK 1062107 A1	06-07-2007
		JP 3772187 B2	10-05-2006
		JP 2004104063 A	02-04-2004
		KR 20040010131 A	31-01-2004
GB 2264589 A	01-09-1993	DE 3938299 A1	28-10-1993
		FR 2688345 A1	10-09-1993
		SE 505057 C2	16-06-1997
		SE 8903839 A	13-04-1994